ON TRANSITION SCENARIOS IN CHANNEL FLOWS

FABIAN WALEFFE

Abstract. [Cha02] has proposed scaling estimates for the magnitude of the smallest perturbations that could trigger turbulence in channel flows. Those estimates are plausible scalings for streak instability but cannot be considered as transition thresholds since feedback is not included. Chapman's analysis also overlooks the modification of the mean shear which can be order one. Here, a Kelvin mode analysis is used to clarify the asymptotics of linear transient growth and the nonlinear generation of streamwise rolls by oblique perturbations is studied explicitly. Implications of the scalings and connections with the self-sustaining process theory are discussed.

1. Introduction

Two transition scenarios related to transient growth have been considered in the literature: (i) the streamwise rolls scenario (SRS) where streamwise rolls create streaks whose possible instability may lead to transition, (ii) the oblique rolls scenario (ORS) where a pair of oblique rolls generate oblique streaks whose nonlinear interaction generate streamwise rolls that may trigger the SRS. A key question has been to estimate the Reynolds number scaling of the smallest perturbation that leads to transition. [TTRD93] conjectured that the scaling was R^a with $a < 1$, strictly, thanks to linear transient growth. An R^{-1} scaling would suggest a nonlinear transition where linear transient amplification does not play a role, since the quadratic nonlinear interaction of an R^{-1} perturbation could directly balance an R^{-1} linear viscous damping.

The numerical simulations of [RSBH98] suggested SRS threshold exponents of $a = -1$ and $-7/4$, and ORS exponents of $a = -5/4$ and $-7/4$, for plane Couette and Poiseuille flow, respectively. However, [Cha02] argues that the true asymptotic exponents are $a = -1$ and $-3/2$ for the SRS and $a = -1$ and $-5/4$ for the ORS.

The ORS, especially the complete model version with 'bootstrapping' necessary for transition ([Cha02, eqns. (2.6-9), fig. 3]), is identical with the scenario studied in [WKH93, Sect. 3]. That scenario was itself a modification of a similar scenario proposed in [BG81] and studied in [JGB86]. The latter references dealt with 'direct resonances', an earlier, and incomplete, version of linear transient growth but went much deeper in their study of nonlinear effects. Surprisingly, most of the later publications studying linear transient growth have limited themselves to calculating maximum linear amplification of perturbation energy, suggesting that this could trigger nonlinear effects, but without actually studying the latter.

[WKH93, Wal95a, Wal95b, Wal97] dismissed scenarios based on linearization about the laminar flow and proposed instead a self-sustaining process (SSP) theory in which R^{-1} streamwise rolls create $O(1)$ streaks whose instability feeds back on the rolls. That theory is now supported by substantial evidence (*e.g.* [HKW95]) and has led to the discovery of traveling wave solutions in plane Couette and Poiseuille flow [Wal98, Wal01, Wal03] and pipe flow [FE03, WK04] as well as time-periodic solutions in plane Couette flow [KK01]. The pipe flow traveling waves appear to be directly connected with 'puffs' [HvDW$^+$04], while the plane flow traveling waves have a structure and preferred scalings (*e.g.* the 100^+ streak spacing) that are very similar to those of the coherent structures observed in the near-wall region of turbulent shear flows. Since these solutions come in pairs, an upper branch and a lower branch, the current thinking mentioned in those references is that the upper branch solutions are 'organizing centers' for turbulent shear flows, a view that is supported by the work of [JKSN05], while the lower branches and their stable manifolds form the boundary separating the basin of attraction of the laminar state from that of the turbulent state ([IT01, WW05]).

The farther-reaching work on transient growth ([RSBH98], [Cha02]) has moved closer to the SSP theory. Those works focus on perturbations that lead to unstable streaks, rather than on perturbations that lead to maximum linear growth of energy. However, Chapman's analysis consists only of scaling estimates for streak

Date: 2005/03/23: PREPRINT.
Key words and phrases. Transition.

instability and does not include feedback. The only certain consequence of the streak instability, *a priori*, is that a nonlinear 'Reynolds stress' will develop to extract energy from the streaks. Thus, the nonlinear effects triggered by the streak instability could simply destroy the streaks and accelerate the return to the laminar flow, rather than trigger transition to a turbulent flow. Of course, work on the SSP has demonstrated that it is possible to have key roll-producing nonlinear interactions in addition to the streak-destroying nonlinear effects, but this is well beyond Chapman's work. His analysis thus provide plausible estimates for streak instability but those cannot be considered as estimates for transition since they do not include feedback.
Chapman's neoclassical analysis involves WKB and matched asymptotics of the linear effects together with scaling arguments for the nonlinear interactions. Here, the linear asymptotics of transient growth are illustrated using a revealing analysis in terms of Kelvin modes and the nonlinear generation of streamwise rolls is studied explictly. The implications of the scaling results for both scenarios are discussed.

2. Governing equations

The Navier-Stokes equations for incompressible flow read

$$\left(\partial_t - \frac{1}{R}\nabla^2\right)\boldsymbol{v} = -\boldsymbol{\nabla} p - \boldsymbol{\nabla}\cdot(\boldsymbol{v}\otimes\boldsymbol{v}), \tag{1}$$

where $\boldsymbol{v}(\boldsymbol{x},t)$ is the divergence-free velocity field at position $\boldsymbol{x}\in\mathbb{R}^3$ and time $t>0$, $p(\boldsymbol{x},t)$ is the kinematic pressure and R is the Reynolds number. The equations have been written in conservative form where $\boldsymbol{v}\otimes\boldsymbol{v}$ denotes tensor product and $\boldsymbol{\nabla}\cdot(\boldsymbol{v}\otimes\boldsymbol{v}) = (\boldsymbol{v}\cdot\boldsymbol{\nabla})\boldsymbol{v}$ since $\boldsymbol{\nabla}\cdot\boldsymbol{v}=0$. Consider plane shear flows and cartesian coordinates with x streamwise, y shearwise and z spanwise and corresponding velocity components u, v, w. A convenient reduction is to project the equations with the operators $\mathcal{P}_\eta(\cdot) = \hat{\mathbf{y}}\cdot(\boldsymbol{\nabla}\times(\cdot)) \equiv [\partial_z, 0, -\partial_x]$ and $\mathcal{P}_v(\cdot) = \hat{\mathbf{y}}\cdot(\boldsymbol{\nabla}\times(\boldsymbol{\nabla}\times(\cdot))) \equiv [\partial_x\partial_y, -(\partial_x^2+\partial_z^2), \partial_y\partial_z]$, where $\hat{\mathbf{y}}$ is the unit vector in the y-direction and the expressions $[\cdot,\cdot,\cdot]$ should be understood as 'row' operators to be dotted with 'column' vectors. This yields two coupled equations for $\mathcal{P}_v(\boldsymbol{v}) = -\nabla^2 v$ and $\mathcal{P}_\eta(\boldsymbol{v}) = \eta$,

$$\left(\partial_t - \frac{1}{R}\nabla^2\right)\nabla^2 v = \mathcal{P}_v\left(\boldsymbol{\nabla}\cdot(\boldsymbol{v}\otimes\boldsymbol{v})\right), \tag{2}$$

$$\left(\partial_t - \frac{1}{R}\nabla^2\right)\eta = -\mathcal{P}_\eta\left(\boldsymbol{\nabla}\cdot(\boldsymbol{v}\otimes\boldsymbol{v})\right). \tag{3}$$

The u and w velocity components follow from $\eta = \partial_z u - \partial_x w$ and v since by solenoidality $\partial_x u + \partial_z w = -\partial_y v$ yielding

$$(\partial_x^2+\partial_z^2)\,u = \partial_z\eta - \partial_x\partial_y v, \tag{4}$$

$$(\partial_x^2+\partial_z^2)\,w = -\partial_x\eta - \partial_y\partial_z v. \tag{5}$$

These equations are easily inverted for periodic boundary conditions in the x and z directions. However, this representation is singular for the mean flow components $\overline{u}(y,t)$ and $\overline{w}(y,t)$, where the overbar denotes an x and z average. For plane shear flow in the x direction we take $\overline{w}(y,t)=0$. The equation for the mean flow $\overline{u}(y,t)$ follows from averaging the NSE over x and z

$$\left(\frac{\partial}{\partial t} - \frac{1}{R}\frac{\partial^2}{\partial y^2}\right)\overline{u} = -\overline{\partial_x p} - \partial_y\overline{uv}, \tag{6}$$

where the average pressure gradient $\overline{\partial_x p}$ is prescribed. In plane Poiseuille flow, $\overline{\partial_x p} = -2/R$ with $\boldsymbol{v}=0$ at $y=\pm1$ yielding the steady laminar solution $\boldsymbol{v} = (1-y^2)\hat{\mathbf{x}}$, while in plane Couette flow $\overline{\partial_x p}=0$ with $\boldsymbol{v}=\pm\hat{\mathbf{x}}$ at $y=\pm1$ and the laminar solution $\boldsymbol{v}=y\hat{\mathbf{x}}$.
Linearizing equations (2) and (3) about the laminar parallel shear flow $\boldsymbol{v}=U(y)\hat{\mathbf{x}}$ yields the Orr-Sommerfeld and Squire equations

$$\left(\partial_t + U\partial_x - \frac{1}{R}\nabla^2\right)\nabla^2 v - U''\partial_x v = 0, \tag{7}$$

$$\left(\partial_t + U\partial_x - \frac{1}{R}\nabla^2\right)\eta = -U'\partial_z v. \tag{8}$$

The *streamwise rolls* equation is key to this discussion. It is the x-average of (2)

$$\left(\partial_t - \frac{1}{R}\nabla^2\right)\nabla^2\overline{v}^x = \partial_z\left(\partial_y^2 - \partial_z^2\right)\overline{vw}^x + \partial_y\partial_z^2\left(\overline{ww}^x - \overline{vv}^x\right), \tag{9}$$

where $\overline{(\cdot)}^x$ denotes an x-average.
Since the problem is homogeneous in the x and z directions, it is convenient to Fourier transform in x and z, *i.e.* consider Fourier mode solutions[1] $v = \hat{v}(y,t)e^{i(\alpha x+\gamma z)}$ and $\eta = \hat{\eta}(y,t)e^{i(\alpha x+\gamma z)}$. This yields the familiar form of the Orr-Sommerfeld and Squire equations

$$\left(\partial_t + i\alpha U - \frac{1}{R}(\partial_y^2 - k^2)\right)(\partial_y^2 - k^2)\hat{v} - i\alpha U''\hat{v} = 0, \tag{10}$$

$$\left(\partial_t + i\alpha U - \frac{1}{R}(\partial_y^2 - k^2)\right)\hat{\eta} = -i\gamma U'\hat{v}, \tag{11}$$

where $k^2 = \alpha^2 + \gamma^2$. It is well-known that these linear equations can produce *transient algebraic growth*. Physically, this arises from the "Orr mechanism" in the v equation. The Orr mechanism is a direct consequence of Kelvin's circulation theorem. Differential advection by the shear flow $U(y)\hat{\mathbf{x}}$ leads to the transient skrinking of material contours initially inclined against the shear and consequent amplification of well-chosen initial velocity to conserve circulation (see *e.g.* [Wal95a, Fig. 1]). Transient growth in the η equation results from the v forcing on the RHS. That forcing is the linearized approximation of the redistribution of streamwise velocity by the perturbation velocity v.

3. WKB analysis of linear transient growth

[Cha02] provides a WKB analysis of the linear transient growth processes. To do so he considers the WKB ansatz[2] [Cha02, Sect. 4.2.2]

$$\hat{v} = Ae^{\phi/\epsilon}, \quad \hat{\eta} = \frac{B}{\epsilon}e^{\phi/\epsilon}, \tag{12}$$

where $\epsilon = (\alpha R)^{-1/3} \ll 1$, and $A = A(y,\tilde{t})$, $B = B(y,\tilde{t})$ and $\phi = \phi(y,\tilde{t})$ are functions of y and the *slow time* $\tilde{t} = \epsilon\alpha t$. At leading order, this yields the *geometrical optics* approximation (eikonal equation) for the phase

$$\phi = \phi_0(y) - iU\tilde{t}, \tag{13}$$

and the *physical optics* approximation for the amplitudes (writing ϕ_y for $\partial_y\phi$, etc.)

$$\phi_y A_{\tilde{t}} = 2iU'A + (\phi_y)^3 A, \tag{14}$$

$$B_{\tilde{t}} = (\phi_y)^2 B - i\frac{\gamma}{\alpha}U'A. \tag{15}$$

Since these are purely temporal evolution equations for A and B and $\phi_y = \phi_0'(y) - iU'\tilde{t}$ is linearly related to $\tilde{t}$, it is convenient to make the change of variable $\tau = U'\tilde{t} + i\phi_0'(y) = i\phi_y$. Then

$$A = A_0(y)\frac{\tau_0^2}{\tau^2}\exp\left(\frac{\tau_0^3 - \tau^3}{3U'}\right), \tag{16}$$

$$B = \left[\frac{i\gamma A_0(y)}{\alpha}\left(\frac{\tau_0^2}{\tau} - \tau_0\right) + B_0(y)\right]\exp\left(\frac{\tau_0^3 - \tau^3}{3U'}\right), \tag{17}$$

which are equivalent to Chapman's (4.28) and (4.29). These solutions blow-up as $\tau \to 0$, but the asymptotics break down for $\tau = O(\epsilon)$. Chapman argues that the growth in A is capped at ϵ^{-2} and in B at ϵ^{-1}. However, B is scaled by a factor ϵ^{-1} in the WKB ansatz (12), so the net amplification in both A and B would be of the same order, namely $O(\epsilon^{-2})$. Chapman also argues that the largest transient growth occurs when $\phi_0(y) = iU\tilde{t}_0$, so that ϕ is pure imaginary and the 'blow-up' time is the same for every y. Note that $\tilde{t}_0 = \epsilon t_0$ must be $O(1)$ to achieve maximum transient growth at a time $t = t_0 = O(\epsilon^{-1})$.

[1] The z-wavenumber, γ, is usually denoted β in the literature.

[2] Chapman picks $\hat{v} = \alpha\epsilon A\exp(\phi/\epsilon)$, $\hat{\eta} = B\exp(\phi/\epsilon)$ but (12) is equivalent and more convenient for discussion of nonlinear effects and comparison with the Kelvin mode analysis.

4. Kelvin mode analysis of transient growth

Equations (10) and (11) for $U(y) = Sy$ with S constant, admit Kelvin mode solutions of the form

$$\hat{v}(y,t) = v(t)e^{i\beta(t)y}, \qquad \hat{\eta}(y,t) = \eta(t)e^{i\beta(t)y}. \tag{18}$$

Substituting these expressions into (10), (11) yields[3]

$$\beta = \beta_0 - \alpha S t, \tag{19}$$

$$\dot{v} + \left(\frac{\beta^2 + k^2}{R} + \frac{2\beta\dot{\beta}}{\beta^2 + k^2} \right) v = 0 \tag{20}$$

$$\dot{\eta} + \frac{\beta^2 + k^2}{R}\eta = -i\gamma S v. \tag{21}$$

Equations (19), (20) and (21) correspond to the leading order WKB equations (13) , (14) and (15), respectively, with $\beta \equiv -i\phi_y/\epsilon$. For the benefit of comparison, let $\tilde{\beta} = \epsilon\beta$ and $\tau = \epsilon(\alpha S t - \beta_0) = -\tilde{\beta}$, then the solutions of (20) and (21) read

$$v = v_0 \frac{\tau_0^2 + \epsilon^2 k^2}{\tau^2 + \epsilon^2 k^2} \exp\left(\frac{\tau_0^3 - \tau^3}{3S} + \epsilon^2 k^2 \frac{\tau_0 - \tau}{S} \right), \tag{22}$$

$$\eta = \left[\frac{i\gamma v_0}{\alpha} \frac{\tau_0^2 + \epsilon^2 k^2}{\epsilon^2 k} \left(\arctan\frac{\tau_0}{\epsilon k} - \arctan\frac{\tau}{\epsilon k} \right) + \eta_0 \right] \exp\left(\frac{\tau_0^3 - \tau^3}{3S} + \epsilon^2 k^2 \frac{\tau_0 - \tau}{S} \right), \tag{23}$$

which tend to the WKB solutions (16), (17) (if we define $\epsilon\eta = B$ as in (12)) as $\epsilon \to 0$.[4] The WKB analysis is somewhat more general since it is formulated for an arbitrary $U(y)$, however the asymptotics require $U' = O(1)$. On the other hand, the Kelvin mode analysis does not break down for small τ, indeed it is valid for any ϵ and for all τ.

Equations (19), (20) indicate that $\dot{v} = 0$ when $(\beta^2+k^2)^2 = 2\alpha R\beta$. A graphical analysis of that equation for β shows that it has two positive roots $\beta_1 \geq \beta_2 > 0$ if R is large enough, with $\beta_1 \sim (2\alpha S R)^{1/3} = \epsilon^{-1}(2S)^{1/3}$ and $\beta_2 \sim k^4/(2\alpha S R) = \epsilon^3 k^4/(2S)$, asymptotically as $R \to \infty$ ($\epsilon \to 0$). The root β_1 corresponds to a minimum of $v(t)$ and β_2 to a maximum. The optimum amplification in (22) therefore occurs at $\tau = -\tilde{\beta} = -\epsilon\beta_2 \sim -\epsilon^4 k^4/(2S)$ for $\tau_0 = -\tilde{\beta}_0 = -\epsilon\beta_1 \sim -(2S)^{1/3}$. The maximum amplification in both $v(t)$ and $\eta(t)$ is indeed $O(\epsilon^{-2})$ in agreement with Chapman's matched asympotic expansions. Plotting (22), (23) provides curves very similar to the numerical channel results shown in fig. 1.

5. Nonlinear generation of streamwise rolls

Consider initial conditions in the form of a pair of oblique modes such that $v = v^+(y,t)e^{i\alpha x}e^{i\gamma z} + v^-(y,t)e^{-i\alpha x}e^{i\gamma z} + c.c.$ with vertical vorticity perturbations $\eta = \eta^+(y,t)e^{i\alpha x}e^{i\gamma z} + \eta^-(y,t)e^{-i\alpha x}e^{i\gamma z} + c.c.$ where $c.c.$ denotes complex conjugate, as in [BG81], [WKH93] and [Cha02]. Our main interest is the generation of streamwise rolls $V(y,t)e^{i2\gamma z} + c.c.$ from the nonlinear interaction between the (α,γ) and $(-\alpha,\gamma)$ modes. From the streamwise roll equation (9), we obtain

$$\left(\partial_t - \frac{1}{R}(\partial_y^2 - 4\gamma^2) \right)(\partial_y^2 - 4\gamma^2)V = 2i\gamma\left(\partial_y^2 + 4\gamma^2\right)\left(v^+w^- + w^+v^-\right) + 8\gamma^2\partial_y\left(v^+v^- - w^+w^-\right), \tag{24}$$

[3] Another approach is to Fourier transform in the y-direction, then $yf(y,t) \to i\partial\hat{f}(\beta,t)/\partial\beta$ and equations (10), (11) become first order PDEs in β, t space whose characteristics are (19).

[4] The exponential factor shows 'shear-induced diffusion', the enhanced viscous decay on a $(\alpha R)^{1/3}$ time scale arising from the linear increase with time of the wavenumber β as a result of the shear.

where $w^\pm = ik^{-2}\left(\pm\alpha\eta^\pm + \gamma\partial_y v^\pm\right)$, from (5), hence the right-hand side of (24) can be written as the sum of three forcing terms, $F_{vv} + F_{v\eta} + F_{\eta\eta}$, where

$$F_{vv} = \frac{8\alpha^2\gamma^2}{k^2}\partial_y(v^+v^-) + \frac{8\gamma^4}{k^4}\partial_y\left(\partial_y v^+\partial_y v^-\right) - \frac{2\gamma^2}{k^2}\partial_y^3(v^+v^-), \tag{25}$$

$$F_{v\eta} = \frac{2\alpha\gamma}{k^2}\left(\partial_y^2 + 4\gamma^2\right)(v^+\eta^- - v^-\eta^+) + \frac{8\alpha\gamma^3}{k^4}\partial_y\left(\eta^+\partial_y v^- - \eta^-\partial_y v^+\right), \tag{26}$$

$$F_{\eta\eta} = -\frac{8\alpha^2\gamma^2}{k^4}\partial_y\left(\eta^+\eta^-\right). \tag{27}$$

Equation (24) and the decomposition (25-27) are identical to [WKH93, eqn. (7)] modulo a difference in the definition of the oblique modes.

Maximum nonlinear interaction requires picking two oblique modes that reach their maximum at the same time. Therefore, from (19), if $\beta_0 \sim (2\alpha SR)^{1/3}$ is the optimum initial β for the (α,γ) mode then $-\beta_0$ should be the initial β for the $(-\alpha,\gamma)$ mode and $\beta^+(t) = -\beta^-(t)$, for all t. The two optimum Kelvin modes then have the form

$$v^\pm(y,t) = v(t)e^{\pm i\beta(t)y}, \qquad \eta^\pm(y,t) = \eta(t)e^{\pm i\beta(t)y}, \tag{28}$$

but one verifies easily that the nonlinear forcings of streamwise rolls (25), (26), (27) vanish identically for such oblique modes. So the nonlinear interaction of two optimally growing Kelvin modes does not generate streamwise vortices.

The WKB analysis suggests the consideration of modulated Kelvin waves of the form

$$v^\pm(y,t) = A_0^\pm(y)a(t)e^{\pm i\beta(t)y}, \qquad \eta^\pm(y,t) = A_0^\pm(y)b(t)e^{\pm i\beta(t)y}, \tag{29}$$

where $a(t)$ and $b(t)$ are the right-hand sides of (22) and (23), respectively, with $v_0 = 1$ and $\eta_0 = 0$. Indeed, for plane Couette flow $U(y) = Sy$, Chapman's WKB analysis leads to $\phi/\epsilon = iSy(\tilde{t}_0 - \tilde{t})/\epsilon = i\alpha S(t_0 - t)y = i(\beta_0 - \alpha St)y$ with $\beta_0 = \alpha St_0 = O(\epsilon^{-1})$. The $A_0(y)$ amplitude modulation implies that the oblique perturbations now consist of a pair of near-optimum wavepackets of Kelvin modes. For optimum oblique perturbations of the form (29), one verifies that

$$F_{\eta\eta} = -b^2(t)\,\frac{8\alpha^2\gamma^2}{k^4}\frac{d}{dy}\left(A_0^+A_0^-\right). \tag{30}$$

is the dominant nonlinear term as expected in [BG81], [JGB86], [Cha02], since $\lim_{t\to\infty}|a(t)|/|b(t)| = 0$, and it appears possible to generate whatever large scale streamwise vortices by choosing the modulating amplitudes $A_0^+(y)$ and $A_0^-(y)$ judiciously. The natural envelopes $A_0^+(y) = A_0^-(y) = \exp(-y^2)$, for which $dA_0^2/dy = -4y\exp(-2y^2)$, would generate a *pair* of counter-rotating vortices, antisymmetric about $y = 0$.

These conclusions are essentially correct, although the WKB expressions (29) are not valid for all times. In particular, for incompressible flow in a channel, the $v = 0$ boundary condition is instantly propagated by the pressure and this leads to $O(1)$ changes in the form of the solution. Indeed, the inviscid ($R^{-1} = 0$) solutions to (10), with $v = 0$ at $y = \pm1$, that correspond to Kelvin modes are

$$\hat{v}(y,t) = v(t)\left[e^{i\beta(t)y} - \cos\beta(t)\frac{\cosh ky}{\cosh k} - i\sin\beta(t)\frac{\sinh ky}{\sinh k}\right], \tag{31}$$

where $\beta(t) = \beta_0 - \alpha St$ and $v(t)$ is (22) without the viscous exponential factor ($\tau = -\epsilon\beta$ so ϵ cancels out from the remainder). Clearly, the modulated Kelvin mode structure (29) is not preserved. The viscous channel problem is studied numerically in the next section.

6. Nonlinear generation of streamwise rolls in a channel

Consider plane Couette flow with $S = 1$ and modulated Kelvin mode initial conditions of the form $\hat{v}(y,0) = A_0(y)\exp(i\beta_0 y)$, $\hat{\eta}(y,0) = 0$ and select $A_0(y) = \cos^5\pi y/2$. The envelope $A_0(y) = \cos^4(\pi y/2)\exp(y^2/(y^2-1))$ that vanishes exponentially as $y \to \pm1$ has also been considered with little difference in the results. This $\hat{v}(y,0)$ is illustrated in fig. 2 for $\beta_0 = (\alpha SR)^{1/3}$ and has a phase $(\alpha SR)^{-1/3}\Im(\log(v)) = y$. The time evolution for such initial conditions is shown by the solid curves in fig. 1. These results are virtually identical to those obtained for the numerically determined 'optimum' initial conditions in [Cha02, Figs. 4,5,7,8] (note that some of those figures are for $R = 10^4$ and others for $R = 10^5$). Similar initial conditions with $\beta_0 = (2\alpha SR)^{1/3}$, the optimum value for a single Kelvin mode, lead to larger amplitudes (dashed curves in fig. 1). It has

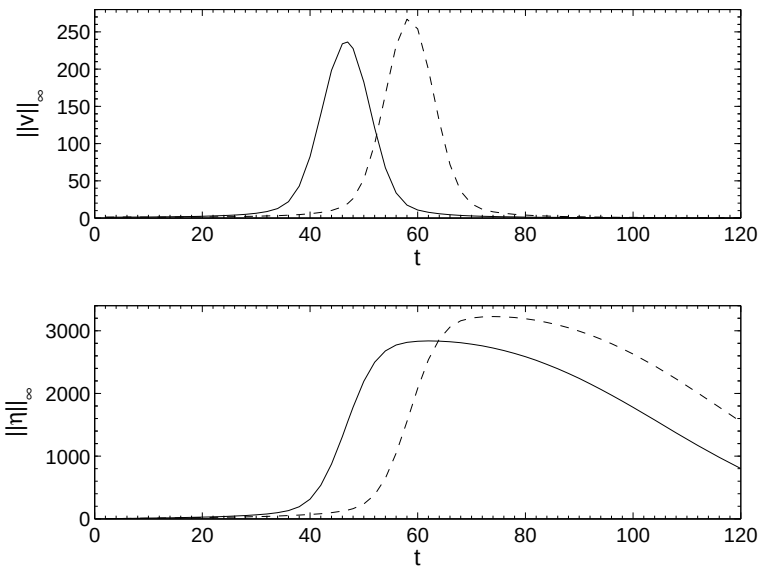

FIGURE 1. Time evolution of maximum over y of $|\hat{v}(y,t)|$ (top) and $|\hat{\eta}(y,t)|$ (bottom) for plane Couette flow with $\alpha = \gamma = S = 1$, $R = 10^5$ and $\beta_0 = R^{1/3}$ (solid), $\beta_0 = (2\,R)^{1/3}$ (dash).

been verified that $\beta_0 = (4\alpha SR)^{1/3}$ leads to less amplification, so $\beta_0 = (2\alpha SR)^{1/3}$ appears to be optimum for the channel as well. Thus $\beta_0 = (\alpha SR)^{1/3}$ and the numerically determined initial conditions in [Cha02] do not lead to the largest amplitudes. This is probably because the latter correspond to maximum energy amplification, not to maximum amplitude. Maximum amplitude, not maximum energy, is of course more relevant for nonlinear effects.

Figure 3 illustrates the structure of $\hat{\eta}(y,t)$ at three different times. Figure 4 shows the structure of $F_{\eta\eta}(y,t)$ at the times of maximum $\|\hat{\eta}\|_\infty$ for both $R = 10^4$ and $R = 10^5$. That $F_{\eta\eta}$ is the (real) streamwise roll forcing corresponding to the nonlinear interaction of a pair of oblique modes with $v^\pm(y,0) = A_0(y)\exp(\pm i\beta_0 y)$, $\eta^\pm(y,0) = 0$ and $A_0(y)$ real, so $v^-(y,t) = (v^+)^*(y,t)$ and $\eta^-(y,t) = -(\eta^+)^*(y,t)$, where $()^*$ denotes complex conjugate. These forcings were computed for $A_0 = \cos^5(\pi y/2)$, $\beta_0 = (\alpha SR)^{1/3}$ and have maximum amplitudes of $1.8\,10^6$ and $5.1\,10^7$ for $R = 10^4$ and 10^5, respectively. The nonlinear forcing for $\beta_0 = (2\alpha SR)^{1/3}$ with the same A_0 have a nearly identical structure but a larger maximum amplitude of $6.6\,10^7$ for $R = 10^5$, as expected.

7. Concluding remarks

References

[BG81] D. J. Benney and L. H. Gustavsson. A new mechanism for linear and nonlinear hydrodynamic instability. *Studies in Applied Mathematics*, 64:185–209, June 1981.

[Cha02] S.J. Chapman. Subcritical transition in channel flows. *J. Fluid Mech.*, 451:35–97, 2002.

[FE03] H. Faisst and B. Eckhardt. Traveling waves in pipe flow. *Phys. Rev. Lett.*, 91:224502, 2003.

[HKW95] J. Hamilton, J. Kim, and F. Waleffe. Regeneration mechanisms of near-wall turbulence structures. *J. Fluid Mech.*, 287:317–348, 1995.

[HvDW+04] Bjorn Hof, Casimir W.H. van Doorne, Jerry Westerweel, Frans T.M. Nieuwstadt, Holger Faisst, Bruno Eckhardt, Hakan Wedin, Richard R. Kerswell, and Fabian Waleffe. Experimental observation of nonlinear traveling waves in turbulent pipe flow. *Science*, 305(5690):1594–1598, 2004.

[IT01] T. Itano and S. Toh. The dynamics of bursting process in wall turbulence. *J. Phys. Soc. Japan*, 70:703–716, 2001.

[JGB86] P. S. Jang, R. L. Gran, and D. J. Benney. On the origin of streamwise vortices in a turbulent boundary layer. *Journal of Fluid Mechanics*, 169:109–123, August 1986.

[JKSN05] J. Jimenez, G. Kawahara, M.P. Simens, and M. Nagata. Characterization of near-wall turbulence in terms of equilibrium and 'bursting' solutions. *Phys. Fluids*, 17:015105 (16pp.), 2005.

[KK01] G. Kawahara and S. Kida. Periodic motion embedded in Plane Couette turbulence: regeneration cycle and burst. *J. Fluid Mech.*, 449:291–300, 2001.

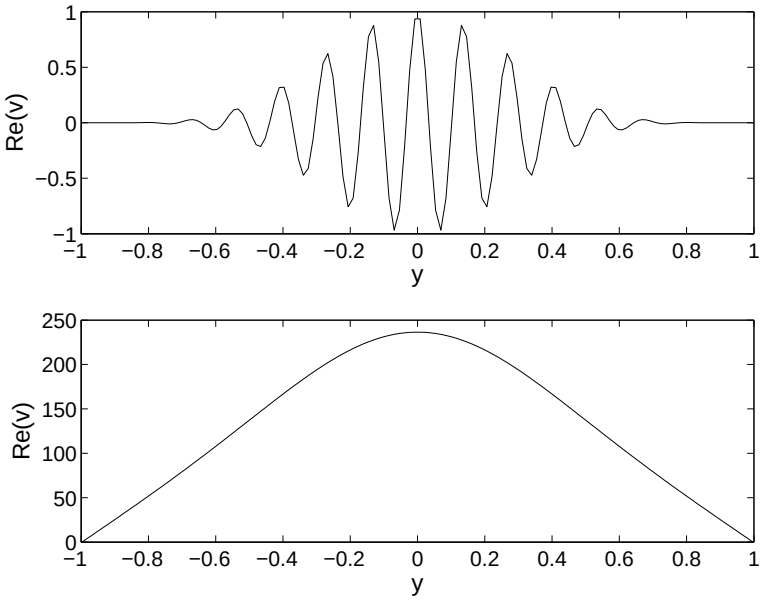

FIGURE 2. Real part of $\hat{v}(y,t)$ at $t = 0$ (top) and $t = 47$ (bottom) for plane Couette flow with $\alpha = \gamma = S = 1$, $R = 10^5$, $\beta_0 = R^{1/3}$.

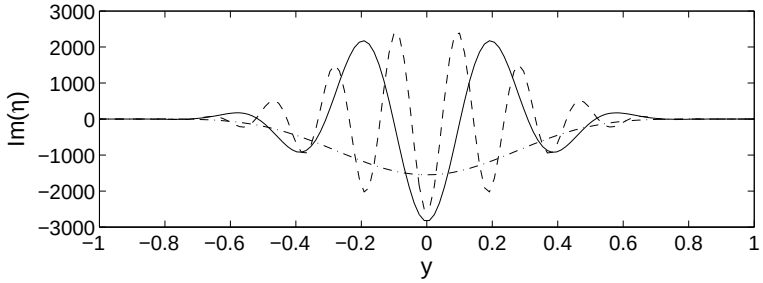

FIGURE 3. Imaginary part of $\hat{\eta}(y,t)$ for $t = 47$ (dash-dot, non-oscillating), $t = 62$ (solid) and $t = 80$ (dash, oscillating) for plane Couette flow with $\alpha = \gamma = S = 1$, $R = 10^5$, $\beta_0 = R^{1/3}$.

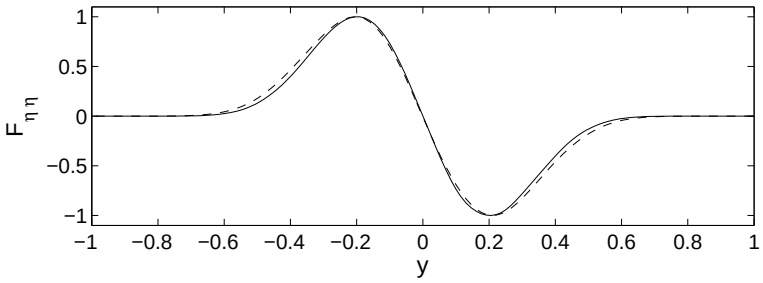

FIGURE 4. Normalized streamwise roll forcing $F_{\eta\eta}$ for $\alpha = \gamma = 1$, $\beta_0 = R^{1/3}$ at time of largest $||\eta||_\infty$: $t = 62$ for $R = 10^5$ (solid) and $t = 32$ for $R = 10^4$ (dash). Maximum $F_{\eta\eta}$ is $1.8\ 10^6$ for $R = 10^4$ and $5.1\ 10^7$ for $R = 10^5$.

[RSBH98] S.C. Reddy, P.J. Schmid, J.S. Baggett, and D.S. Henningson. On stability of streamwise streaks and transition thresholds in plane channel flows. *J. Fluid Mech.*, 365:269–303, 1998.

[TTRD93] N. Trefethen, A.E. Trefethen, S.C. Reddy, and T.A. Driscoll. Hydrodynamic stability without eigenvalues. *Science*, 261:578–584, 1993.

[Wal95a] F. Waleffe. Hydrodynamic stability and turbulence: Beyond transients to a self-sustaining process. *Stud. Applied Math.*, 95:319–343, 1995.

[Wal95b] F. Waleffe. Transition in shear flows: Nonlinear normality versus non-normal linearity. *Phys. Fluids*, 7:3060–3066, 1995.

[Wal97] F. Waleffe. On a self-sustaining process in shear flows. *Phys. Fluids*, 9:883–900, 1997.

[Wal98] F. Waleffe. Three-dimensional coherent states in plane shear flows. *Phys. Rev. Lett.*, 81:4140–4148, 1998.

[Wal01] F. Waleffe. Exact coherent structures in channel flow. *J. Fluid Mech.*, 435:93–102, 2001.

[Wal03] F. Waleffe. Homotopy of exact coherent structures in plane shear flows. *Phys. Fluids*, 15:1517–1543, 2003.

[WK04] H. Wedin and R.R. Kerswell. Exact coherent structures in pipe flow. *J. Fluid Mech.*, 508:333–371, 2004.

[WKH93] F. Waleffe, J. Kim, and J. Hamilton. On the origin of streaks in turbulent shear flows. In F. Durst, R. Friedrich, B.E. Launder, F.W. Schmidt, U. Schumann, and J.H. Whitelaw, editors, *Turbulent Shear Flows 8: selected papers from the Eighth International Symposium on Turbulent Shear Flows, Munich, Germany, Sept. 9-11, 1991*, pages 37–49. Springer-Verlag, Berlin, 1993.

[WW05] F. Waleffe and J. Wang. Transition threshold and the self-sustaining process. In T. Mullin and R.R. Kerswell, editors, *Non-uniqueness of Solutions to the Navier-Stokes Equations and their Connection with Laminar-Turbulent Transition*, pages 85–106. Kluwer, 2005.

Departments of Mathematics and Engineering Physics, University of Wisconsin, Madison, WI 53706, and CNLS, CCS-2 and IGPP, Los Alamos National Laboratory, Los Alamos, NM 87544
E-mail address: waleffe@math.wisc.edu